Nonparametric estimation of ultrasound pulses

Jensen, Jørgen Arendt; Leeman, Sidney

Published in:
I E E E Transactions on Biomedical Engineering

Link to article, DOI:
10.1109/10.324524

Publication date:
1994

Document Version
Publisher's PDF, also known as Version of record

Nonparametric Estimation of Ultrasound Pulses

Jørgen Arendt Jensen and Sidney Leeman

Abstract— **An algorithm for nonparametric estimation of 1-D ultrasound pulses in echo sequences from human tissues is derived. The technique is a variation of the homomorphic filtering technique using the real cepstrum, and the underlying basis of the method is explained. The algorithm exploits *a priori* knowledge about the structure of rf line echo data and can employ a number of adjacent rf lines from an image. The prime application of the algorithm is to yield a pulse suitable for deconvolution algorithms. This will enable these algorithms to properly take into account the frequency dependence of the attenuation and its variation within a patient and among patients. It is also possible to use the estimated pulse for attenuation estimation, and the consistency of the assumptions underlying the proposed technique is demonstrated by its ability to recover low variance attenuation estimates in the normal liver from *in vivo* pulse-echo data. Estimates are given for eight different patients.**

I. Introduction

IN MEDICAL ultrasound, a pulsed field is transmitted into the body, and the "echoes," back-scattered towards the emitting transducer, are detected as a 1-D voltage trace, the rf line. Physical modeling of the pulse-echo loop is quite complex, even if simplifying assumptions are made about the transducer excitation, the properties of tissue, and the characteristics of the scattering interactions [1], [2]. Much of the resultant complexity arises from the three (spatial)-dimensional nature of the entities involved, viz. the incident pulse, the scattering tissue, and the scattered wave field.

Rather than attempting to detail the full 3-D scattering problem, it has proved fruitful to model the rf line directly, as being, in some way, the result of combining a hypothetical 1-D "pulse" with a hypothetical 1-D tissue. This is a common, often implicit, assumption made in attenuation estimation [3] and deconvolution [4], [5], and is also used in Doppler ultrasound systems [6], [7]. Thus, it is commonly assumed that the received pulse-echo signal may be expressed as a depth-dependent pulse convoluted with a tissue reflectivity function. In such models, both the pulse amplitude and shape are dependent on depth in tissue. This results from the frequency-dependent attenuation processes, which lead to the observed nonstationarity of the special properties of the rf line from tissue (as revealed by short-time Fourier analysis, for example).

Manuscript received April 15, 1991; revised June 17, 1994. The research was partly funded by the Danish Technical Research Council, grant 16-4218E, Brüel and Kjær A/S, Novo's Foundation, H. C. Ørsteds Foundation and Trane's Foundation.

J. A. Jensen is with the Electronics Institute, Technical University of Denmark, DK-2800 Lyngby, Denmark.

S. Leeman is with the Department of Medical Engineering and Physics, Dulwich Hospital, King's College, London SE22 8PT, UK.

IEEE Log Number 9404280.

Several authors have devised techniques to enhance the resolution of ultrasound images via deconvolution algorithms. They ultimately rely on knowledge of a pulse, which, in practice, would have to be first estimated from the data [8], [9]. Since pulse estimation may be regarded as a more fundamental problem, inasmuch as it also provides part of the input to deconvolution routines, the work described below is concerned solely with aspects related to pulse estimation. The estimated pulse can, however, also be of use as the input to other algorithms. For obvious reasons, the tissue reflectivity function is occasionally referred to as the tissue impulse response. A knowledge of this is required for quantitative scattering methods such as impediography, as well as in some structural tissue characterization techniques [10]. On the other hand, measuring depth dependent changes in the pulse characteristics is required for virtually all pulse-echo attenuation estimation techniques [11]–[13]. The attenuation should, thus, be reflected in the estimated pulse; that this is the case is demonstrated in Section IV.

Several authors have devised algorithms for estimating ultrasound pulses. AR-models have been used by Towfig *et al.* [14] and Kuc and Li [12]. Jensen [2] used an ARMA model for the pulses. The work presented here does not use a parametric model, and, as such, does not introduce restrictions enforced on the pulse by such models. Less *a priori* knowledge is needed, as a model is not necessary. Only a cepstral cut-off must be determined, and this can be found from the actual data used.

The paper proceeds along the following line: Section II gives a derivation of the algorithm. It employs homomorphic signal processing and can utilize data from multiple rf lines by averaging them in the cepstral domain. The appearance of the pulse is determined by a cepstral cut-off, and guide lines for choosing this is given. Section III gives various examples of use. First the effect of using multiple lines is shown, and then the algorithm is employed on *in vivo* data. Section IV finally gives results from using the approach to estimate attenuation. Low variance estimates are obtained, if a sufficient amount of data is used.

II. Derivation of the Algorithm

It is possible to specify a number of constraints, or "consistency conditions," which limit the ranges of choice for both the pulse- and tissue-functions, when modeling or simulating the rf line as a generalized convolution [15]. It is reasonable to expect that the overall character of the pulse should not be too unlike the (1-D) pulse-echo signal obtained as the echo from a planar reflector orthogonal to the beam in a water tank. This constraint will be interpreted to imply that, in general, the amplitude spectrum of the pulse is quite smooth and sharply

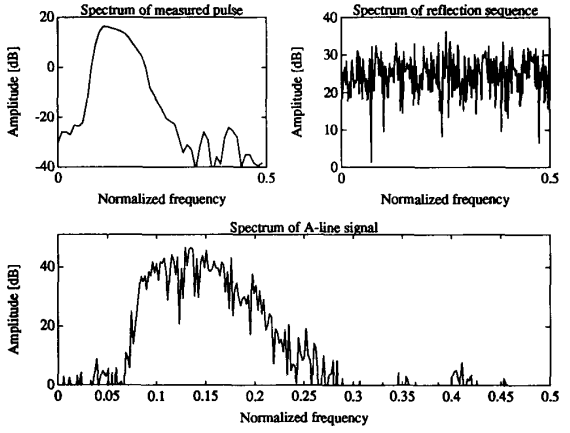

Fig. 1. Spectra of measured pulse and synthetic reflection signal.

peaked about a value not too far removed from the nominal center frequency of the transducer. To account for attenuation effects, the mean frequency and amplitude of the pulse should decrease progressively with distance: this, in turn, implies that the (model) pulse should vary smoothly with depth.

The amplitude spectrum of a typical *in vivo* rf line is very "spiky," exhibiting a great deal of structure, which is generally ascribed to the intricate nature of the interrogated tissue. Thus, it is not unreasonable to expect that the amplitude spectrum of the (1-D) tissue reflectivity function be of similar behavior. Note that this property is enforced by the expectation that the pulse spectrum be relatively smooth. Not quite so obvious is the requirement that the spectrum of the tissue reflectivity function be considerably more wideband than that of the pulse. This follows from the observation that spiky spectra are always observed (attenuation allowing) for the rf line from tissue, even when interrogating by pulses with central frequencies that straddle the entire diagnostic frequency range, and whose bandwidths do not overlap.

It is instructive to examine the structure of a pulse estimation algorithm within the specific framework of a simple, statistically stationary model whereby the (sampled) rf line, $y(k)$, is synthetically generated as a convolution between a random "tissue" reflection sequence e and a realistic, known, 1-D pulse p

$$y = p * e \tag{1}$$

where $*$ denotes convolution.

In the simulation presented in Fig. 1, the pulse spectrum was chosen to be that of the measured echo from a thick planar perspex target oriented orthogonally to the acoustic axis of a commercial Brüel and Kjær 3 MHz (nominal) transducer, and located at the nominal focus (150 mm). The transducer diameter was 16.2 mm. Measurements were conducted in a water tank, with the echoes digitized at 20 MHz to nominal 8 b accuracy by a LeCroy 9450 oscilloscope. A Brüel and Kjær 1846 scanner was used for driving the transducer and amplifying the received response.

A number of points can be noted. The spectrum of the pulse is smooth and band limited. This is to be expected as a transducer is an electromechanical resonant device that can be described well by a relatively simple model with a few degrees of freedom [16], [17]. The tissue reflection sequence is a complex signal with numerous spikes and dips due to the complex underlying structure of the tissue. The sequence used here is a white, Gaussian signal with zero mean. Such a signal could emanate from a tissue region, where speckle is observed in the image. As the signal comes from scattering by numerous small structures, it would, by the law of large numbers, be Gaussian. The resulting line has a mixture of properties from both signals. It is band limited and has a jagged appearance due to the statistical nature of the reflection sequence.

To extract the pulse from the rf line signal, it is necessary to smooth the rapid fluctuations in the spectrum of the latter, in order to recover the smooth bandlimited spectrum of the former. Thus, in essence, a pulse estimation technique should effectively lowpass filter the spectrum of the rf line signal to obtain a smooth function. Indeed, one approach to the problem attempts to implement such a smoothing directly [15]. However, a more sound approach, which seems virtually tailored for the problem in hand, appears to be that based upon homomorphic signal processing [18], [19]. A close variant of this technique is pursued here.

The synthetic rf line signal is, written in the Fourier domain

$$Y(f) = P(f) \cdot E(f). \tag{2}$$

Upper case letters denotes the Fourier Transform of the corresponding lower case letter.

The pulse spectrum is multiplied by the spectrum of the reflections. In order to separate the two, the logarithm is taken

$$\begin{aligned} \log Y(f) &= \log[P(f) \cdot E(f)] \\ &= \log P(f) + \log E(f) \\ &= \log |P(f)| + j\arg\, P(f) \\ &\quad + \log |E(f)| + j\arg\, E(f). \end{aligned} \tag{3}$$

Let us for a moment only consider the amplitude

$$\log |Y(f)| = \log |P(f)| + \log |E(f)|. \tag{4}$$

The log amplitude spectrum of the output signal is the log amplitude spectrum of the pulse perturbed by the spectrum of the reflection sequence. This is visualized in Fig. 1, where the log spectra of pulse, reflections and rf line are shown. Using the properties of log spectra described previously, it is possible to estimate the pulse spectrum by filtering the log amplitude spectrum. In order to do the separation, the Fourier transform of the log amplitude spectrum is calculated. This is called the cepstrum of a signal. Cepstra of the synthetic signals are shown in Fig. 2. The log of the cepstra has been taken so details can be studied. The cepstrum of the pulse contains most of its energy at the first samples, whereas the cepstrum of the reflection signal has an even distribution over the whole range of the cepstrum as expected. Inspecting the log cepstrum of the rf line also reveals more energy at the first samples, which can be ascribed to the pulse. So taking only the first samples of the cepstrum, where the pulse is dominating, and inverse

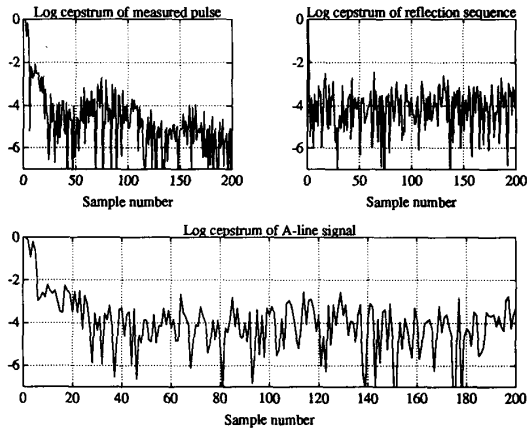

Fig. 2. Log cepstra of measured pulse and synthetic reflection signal.

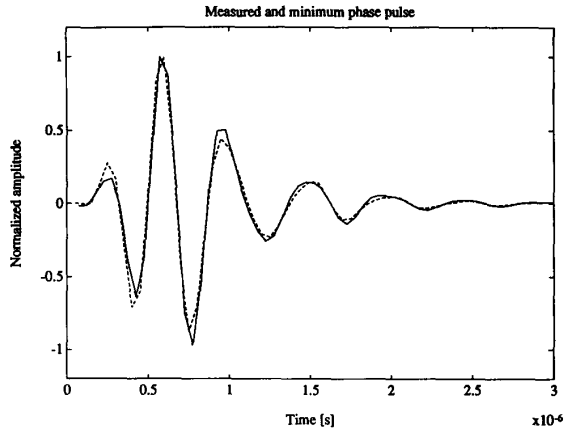

Fig. 3. Pulse from a 3 MHz transducer (—) and the minimum phase version of it (- - -).

Fourier transforming recovers, to a reasonable approximation, the amplitude spectrum of the pulse only.

The choice of cepstrum cut-off, N_c, is determined by the fastest change in the log spectrum that can be ascribed to the pulse. Usually this is the first uprising flank of the spectrum. Reading of the "rise-time" in normalized frequency, $\Delta f/f_s$, and taking the inverse directly yields the sample number where the cut-off should be made. The procedure is equivalent to finding the rise time for a square wave passed through a linear system. The time span of the line from 10% to 90% of the maximum amplitude value is equal to the rise time, and gives an indication of the bandwidth of the linear system as $t_r \approx 1/B$. In this approach, the span is found in the frequency domain of the log amplitude spectrum and determines the upper cut-off of the quefrency. Note also that this cut-off can be determined directly from the data used. This is done by plotting the log-amplitude spectrum, and then fitting a line from the 10% to 90% point of the maximum amplitude for the first rising flank by hand to the data. The cut-off can then be roughly determined. The estimate can be improved by averaging segments of data in order to smooth the spectrum. Although such a technique can provide only an approximate value for the cut-off, it will be demonstrated later that it is sufficiently accurate for practical purposes. It should also be noted that the cepstral cut-off is determined for the transducer type once, and that it can be used for different situations, due to the fact that the *shape* of the spectrum does not change dramatically due to attenuation in tissues. This makes the determination of N_c comparable to determining, e.g., the sampling frequency or the model order for parametric models.

The next question then is how to obtain the phase of the pulse. The phase of the rf line is random and, as it is a Gaussian signal, can not give any phase information, so *a priori* knowledge must be used. A common and fairly reasonable approach is to assume the pulse to be minimum phase. This is equivalent to saying that as much as possible of the energy is concentrated as early as possible in the pulse. Whether this is reasonable can be assessed by comparing a measured pulse to its minimum phase counterpart. An example for a response measured from a 3 MHz transducer, when directed towards a perspex plate, is shown in Fig. 3, along with its minimum phase version. The differences are minute and the minimum phase assumption seems, in this instance, appropriate.

For a minimum phase pulse the amplitude and phase spectrum form a Hilbert transform pair [18]. The spectrum of the minimum phase pulse can thus be found by setting the cepstrum for negative time to zero. If the cepstrum of the log amplitude spectrum is denoted by $C_p(n)$, then the complex cepstrum for the minimum phase signal is

$$C_{pi}(n) = \begin{cases} C_p(n), & n = 0 \\ 2C_p(n), & 1 \leq n \leq N/2 \\ 0, & N/2 < n \leq N-1. \end{cases} \quad (5)$$

A derivation of this result can be found in [18].

In general, the estimate of the cepstrum will be based on a segment of the rf line data. Taking out a segment will have the side effect that reflections before the segment will appear in the segment due to the length of the pulse, and reflections at the end of the segment will be cut-off. A window function should, therefore, be multiplied on the data to remedy these end effects. This will also improve the estimate of the log-spectrum [18].

The full algorithm can now be given. A signal segment is denoted by a lower case letter in the time domain, i.e., y, and upper case letters denote signals in the spectral and cepstral domains. Individual samples are denoted as $e(n)$. $\mathcal{F}$ denotes Fourier transformation and $\mathcal{F}^{-1}$ inverse Fourier transformation. N_c is the sample where the cepstrum should be cut-off in order to get the pulse, and N is the total number of samples in the rf line, y. w is the window used, and the recovered pulse is denoted by p. The algorithm reads

$$\begin{aligned} Y_l &= \log|\mathcal{F}\{y \cdot w\}| \\ C_y &= \mathcal{F}^{-1}\{Y_l\} \\ C_p &= \begin{cases} C_y(n), & n = 0 \\ 2C_y(n), & 1 \leq n \leq N_c \\ 0, & N_c + 1 < n \leq N-1 \end{cases} \\ Y_p &= \mathcal{F}\{C_p\} \\ p &= \mathcal{F}^{-1}\{\exp(Y_p)\}. \end{aligned}$$

In B-scan images, a number of rf lines are acquired. It is reasonable to assume that the pulse in adjacent lines is the same, so an average pulse can be found for a number of lines. This can be accomplished by averaging cepstra from a number of lines. Denoting $C_p^{(i)}$ the cepstrum of the ith line and M the number of lines, the averaged multi-rf line cepstrum is

$$\overline{C}_p = \frac{1}{M}\sum_{i=1}^{M} C_p^{(i)}. \tag{6}$$

Then $\overline{C}_p$ is used instead of C_p in the recovery of the pulse. A decrease in variance of the estimate is then obtained. The decrease will be less than $1/M$, as adjacent rf lines are correlated.

A program written in the Matlab language performing the whole multichannel procedure is shown in Appendix A. It uses a Hamming window on the data and this window is also used throughout this paper.

The amplitude of the pulses estimated will be determined by the scattering strength of the tissue. As the pulse amplitude cannot be separated from the scattering strength, a method to fix the amplitude of the pulse is needed. This can be done by setting $C_p(0)$ to zero, but then the out-off band noise will severely influence the amplitude. A more consistent method is to normalize the pulses so the largest peak in the pulse always is one. This is the method preferred in this paper.

III. Examples of Use

In this section, various examples of use of the single and multichannel algorithm will be shown. Examples are presented for synthetic data, and results obtained from clinical *in vivo* liver data are given in Section III.B.

A. Synthetic Data Examples

The cepstral cut-off N_c must be determined before the algorithm can be used. This can be found from the log amplitude spectrum as explained previously. To show the dependence of the pulse shape on N_c, a synthetic example was generated as

$$y = p * e + n \tag{7}$$

where p is the pulse, e the Gaussian distributed reflections, n the white noise added and y the measured signal.

The signal-to-noise ratio is defined as

$$\text{SNR} = \sqrt{\frac{E[y(k)^2]}{E[n(k)^2]}} \tag{8}$$

where E is the expectation.

The pulse was measured as the response from a 3 MHz Brüel and Kjær 8529 transducer when directed towards a perspex plate. The sampling frequency was 20 MHz, and 512 samples were generated for the rf line. The best value of N_c is approximately 20. The pulses estimated from using 15, 20, 25 and 30 compared to the true pulse is shown in Fig. 4. As

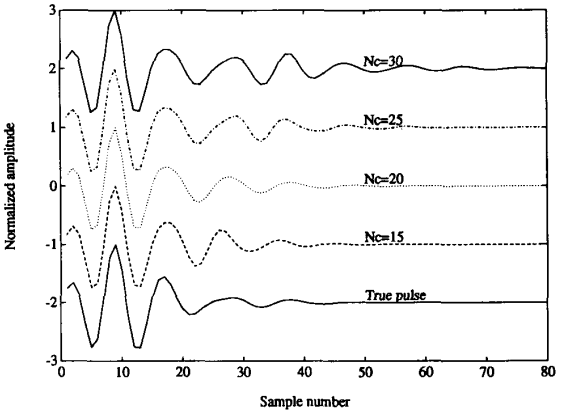

Fig. 4. Pulse estimated from a synthetic rf line when N_c was 15, 20, 25 and 30. The lowest pulse is the true one.

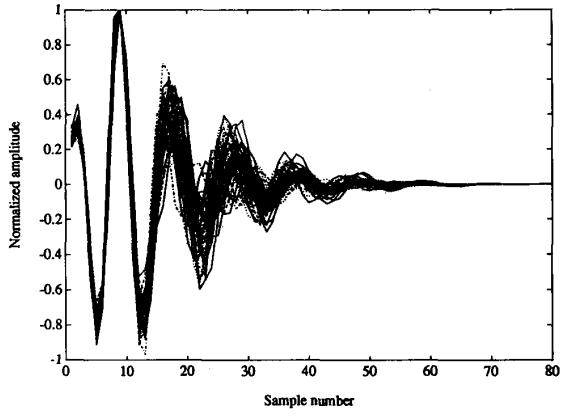

Fig. 5. Fifty pulses estimated from synthetic rf lines with SNR = 30.

can be seen, the choice of N_c is not critical. A value of 20 will be used throughout the rest of the paper.

The capability of the algorithm to estimate pulses for synthetic data will now be shown. The synthetic rf line generated by (7) was used with SNR equal to 30. Fifty different realizations of the reflections and the noise were made and the pulse estimated for each of the lines is shown in Fig. 5.

The mean and variance of the pulses are calculated by

$$\overline{p}(k) = \frac{1}{N_p}\sum_{i=1}^{N_p} p_i(k) \tag{9}$$

$$\sigma^2(k) = \frac{1}{N_p - 1}\sum_{i=1}^{N_p}(p_i(k) - \overline{p}(k))^2. \tag{10}$$

N_p is the number of pulses and p_i is the i-th pulse. The mean $\pm$ three standard deviations are shown in Fig. 6. The correspondence between the true and recovered mean pulse is striking.

The multichannel version uses a number of rf lines. The mean pulse shown in Fig. 7 is estimated when using 10 rf lines and repeating the experiment 50 times. As more data enters the estimation, the variance is decreased correspondingly.

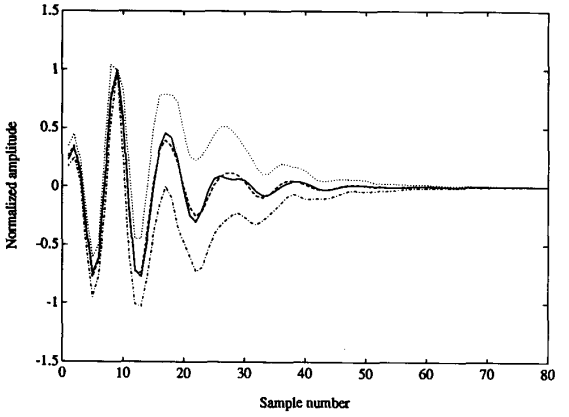

Fig. 6. Mean of the pulses from Fig. 5, with limits equal to ± three standard deviations. Solid line is the true pulse.

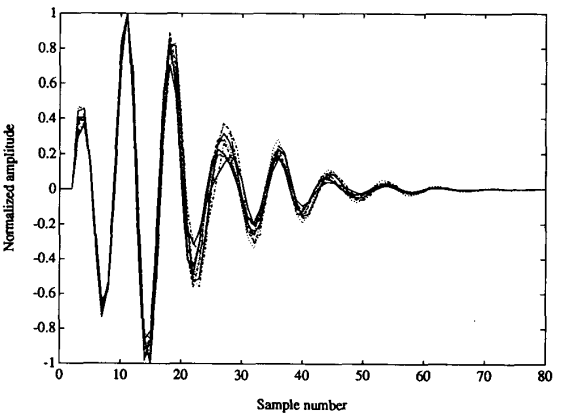

Fig. 8. Ten pulses estimated from *in vivo* liver data.

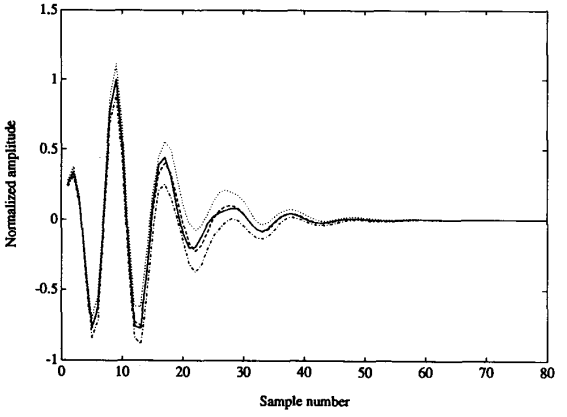

Fig. 7. Mean of pulses estimated by the multichannel algorithm. Limits equal to ± three standard deviations. Solid line is the true pulse.

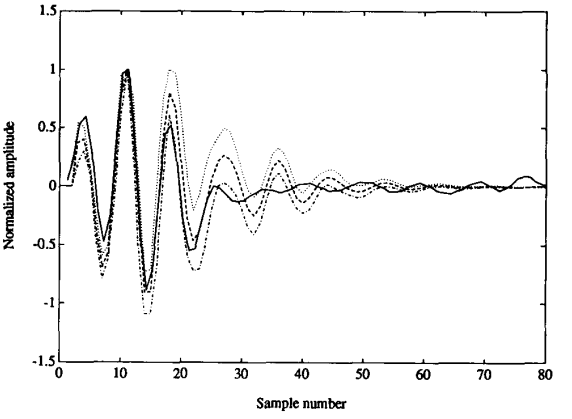

Fig. 9. Mean of pulses estimated *in vivo* by the multichannel algorithm. Limits equal to ± three standard deviations.

The rf lines in a B-mode image are correlated in the lateral direction so the improvement in variance of a full factor of M is not obtained. The factor will be less than M and depends on the correlation of adjacent lines. Note that the averaging of lines does not necessitate a coherent data acquisition, as only the cepstra of the amplitude spectra are averaged.

B. In Vivo Experiments

The multichannel pulse estimator was also tested on clinical data. They were acquired by our sampling system and program system described in [20]–[23]. The sampling system was connected to a Brüel and Kjær 1846 ultrasound scanner with a 3 MHz 8529 sector scan transducer. The data were acquired from eight humans with presumed normal liver function. The liver and right kidney were scanned. The first example is from a 29 year old male. The pulses were estimated from liver data at a depth of 8 cm from the transducer. Ten lines consisting of 512 samples were used for each pulse estimated. Ten pulses were estimated with an overlap of 50% between adjacent 10 line blocks. The result is shown in Fig. 8. The mean pulse ± three standard deviations is shown in Fig. 9. The pulse from the transducer was measured as the reflection from a planar reflector placed at the focal point. The measurement was performed in water, so for comparison the pulse was attenuated by 0.65 dB/[MHz cm], and the minimum phase version of this pulse is shown as the solid line in Fig. 9.

The shape of the "true" pulse inside the liver is unknown, but these results indicate that a plausible 1-D pulse can indeed be consistently recovered from *in vivo* pulse echo data. The mean pulse and the measured pulse are, for the first part of the pulses, quite alike. Problems are encountered at the end of the pulse where the estimated pulses are longer. It should, however, be noted that even the reference pulse is encumbered with uncertainty.

IV. Consistency of Pulse Estimation

It has been pointed out above that a necessary consistency condition imposed on the 1-D equivalent pulse in a realistic convolution model for the *in vivo* rf line is that its mean frequency should exhibit a decline with depth into tissue. This change in pulse shape is assumed to be consistent with the attenuation characteristics of the tissue: indeed, pulse estimation techniques are considered to be a valid approach

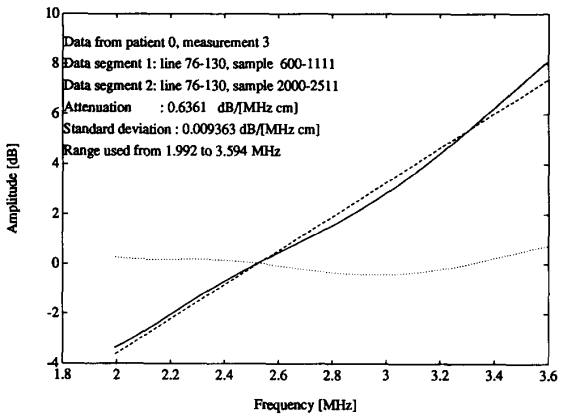

Fig. 10. Attenuation estimated by spectral difference of spectrum of two estimated pulses found by the multichannel algorithm. — is the spectral difference, - - - the fitted line and ··· is the difference between the two.

towards assessing features of such a tissue property [11]. It will be noted that the effects of attenuation are not explicitly written into the pulse recovery algorithm, and it follows that the consistent recovery of attenuation parameters from *in vivo* data provides a sensitive test of methodology developed here.

A common parameterization used for describing the frequency dependence of the attenuation in uniform, isotropic human tissues is the "linear-with-frequency" model

$$\alpha(f) = \alpha_1 f + \alpha_0 \tag{11}$$

where $\alpha(f)$ denotes the (linear) attenuation coefficient and α_1 and α_0 are constants. In nonuniform tissues, the attenuation coefficient, and thus both α_1 and α_0, become functions of position. The change in pulse shape, with depth into tissue, is influenced by the magnitude of α_1 alone. Given that pulse normalization is built into the pulse recovery algorithm, it is clear that only α_1 can be estimated by the technique presented here. α_1 is commonly referred to as the "attenuation slope" and expressed in dB/[cm MHz]; this is the convention we shall adopt below.

The frequency slope of the attenuation of the liver is estimated by finding the pulse at two different depths and then subtracting the spectra and fitting the model.

An example of this approach using the multichannel algorithm is shown in Fig. 10. Between 1.9 and 3.7 MHz, a near linear with frequency attenuation is seen. The spectra were obtained by using 65 lines and 512 samples per line, and then estimating the pulse and plotting the spectral difference from two depths (data segments starting at 2.3 and 7.7 cm and both consisting of 512 samples). The slope was found by fitting a straight line with a least squares fit in the interval between 1.9 and 3.7 MHz. The frequency interval consists of the points in the spectra which are less than 20 dB below the maximum. The procedure for the attenuation estimation is described in Appendix B. By this, the attenuation was determined to be 0.65 dB/[MHz cm] ± 0.01 dB/[MHz cm].

Repeating the experiment for seven other livers gives the values shown in Table I. The first column in the table identifies the patient and the measurement on the patient, as it is indicated in our data base of clinical measurements. All these patients are considered normal, as no abnormalities have previously been detected. The third column gives the number of lines used in the estimation. They were determined manually as the largest area at 2.3 and 7.7 cm from the transducer where a homogeneous liver section could be selected in the image. The last column is the estimated standard deviation from Appendix B. The selection of a homogeneous region ensures that no dominant specular reflections are present in the data. The presence of two specular reflectors separated by less than a pulse length might distort the spectrum. The procedure has also been tried on regions covering specular reflections from blood vessels and this does not seem to create problems. The one situation where problems are encountered is for regions with very strong reflectors that will overload the input amplifiers in the scanner. This is, e.g., encountered at the diaphragm, and is the reason for selecting a homogeneous liver region. The problem with overloading can be solved by employing adaptive time-gain compensation during data acquisition.

TABLE I
ATTENUATION SLOPE VALUES FOUND FROM *IN VIVO* MEASUREMENTS ON EIGHT HUMAN LIVERS

Patient identification	Age years	Lines used	Attenuation dB/[MHz cm]	Std. dB/[MHz cm]
Pat. 0, meas. 3	28	65	0.65	0.0092
Pat. 1, meas. b	28	28	0.58	0.019
Pat. 2, meas. 3	29	65	0.54	0.021
Pat. 13, meas. 4	36	39	0.78	0.011
Pat. 14, meas. 3	48	52	0.53	0.018
Pat. 15, meas. 3	30	65	0.73	0.011
Pat. 16, meas. a	26	51	0.54	0.021
Pat. 17, meas. 3	44	41	0.61	0.020

Note that the multichannel algorithm leads to a good (i.e., low variance) estimate of an attenuation slope for any particular patient, but that the patient-to-patient variation is quite large. The mean value of the estimated standard deviation is 0.016 dB/[MHz cm], whereas the standard deviation of the estimated values is 0.094 dB/[MHz cm], a factor of 5.7 larger than the mean standard deviation. However, such behavior is in accord with the findings of other studies [24]. Moreover, the estimated values for the attenuation slope are generally within the range reported for a normal liver, as measured by a variety of techniques [25], [26]. It is not accurately known to what degree various factors influence the attenuation of "normal" liver: age, sex, level of activity (time of day, contents of, and time elapsed since, last meal), and degree of (even moderate) alcoholic intake, may all be reasonably presumed to have some bearing on the attenuation value. Since the aim of this particular series of measurements was to establish the internal consistency of the pulse estimation technique—as adequately confirmed by the low variance of the attenuation slope estimates for each individual patient—no attempt was made to monitor, or control, all possible attenuation modifying influences (although the age and sex of the patients were noted).

It should be emphasized that a considerable amount of data were involved in the attenuation slope estimates, and that the

results, although very satisfactory, do not necessarily imply superiority over other techniques, such as that suggested by Kuc [3]. Attenuation slope estimation was performed only to demonstrate that the pulse estimation technique is capable of performing consistently and reliably with an adequate quantity of *in vivo* data.

V. Conclusion

It has been demonstrated that it is indeed possible to consistently estimate an equivalent 1-D pulse from *in vivo* ultrasound pulse-echo data. The technique is derived from homomorphic filtering, and relies for its success on the validity of a number of assumptions about the underlying nature of the rf line. The good results obtained in practice imply that these model assumptions are quite appropriate.

It is interesting to observe that the recovered pulse (in liver) has a shape not too unlike that of the echo from a planar reflector properly attenuated. Moreover, the shape changes with depth in liver are consistent with those expected for a frequency dependent attenuation, rising approximately linearly with frequency.

There is a reduction in the variance of the estimate, if the number of input rf lines is increased. The main application for the algorithm is for obtaining the pulse entering a nonparametric deconvolution algorithm like Wiener filtering. It is then possible to track the change in pulse shape due to attenuation, and thereby more accurately compensate for the loss in attenuation. Another application of the proposed technique may well be for attenuation estimation. At present, this looks likely only for relatively large, homogeneous organs such as the liver.

Appendix A
A Matlab Program

The small Matlab program below implements the full one channel and multichannel algorithms. Data are given as a matrix in which each row is an rf line. The pulse is returned in a vector with a length equal to the number of samples in each rf line.

The program should be fairly easy to read. Each variable denotes a vector or matrix and all operators work as matrix operators. A further description of the Matlab language can be found in [27] or other corresponding manuals.

```
%   Estimation of a pulse by homomorphic
%   filtering using a number of rf lines.
%
%  Calling: pulse = homo_2d (y, nc);
%
%        y = The input data.
%        nc = Cepstral cut-off
%      pulse = The estimated pulse
%
%  Version 1.00, 24/9-90 J. A. Jensen

function pulse = homo_2d (y, nc);
[N_lines N_samples]= size(y); % Determine
                                size of image
win = hamming(N_samples)'; % Make a window

% Make a complex cepstrum from all the lines

cepstrum(N_samples) = 0;
for i = 1:N_lines
  log_dft = log(abs(fft(y(i,:).*win)));

  % Calculate the cepstrum

  cepstrum = cepstrum + real
             (ifft(log_dft)/N_lines);
  end;

  % Filter the cepstrum

cep = [cepstrum(1) 2*cepstrum(2:nc)
       zeros(1,N_samples-(nc+1))];
pulse = real(ifft(exp(fft(cep))))';
end;
```

Appendix B
Estimation of Attenuation

The attenuation of the pulse can be determined by fitting the linear with frequency model

$$\alpha(f) = \alpha_1 f + \alpha_0 \tag{12}$$

to the log amplitude spectral difference of two pulses estimated at different depths in tissue.

If y is the discrete spectral difference, then we can write

$$\begin{aligned} y(k) &= \theta^T \varphi(k) \\ \theta^T &= [\alpha_1, \alpha_0] \\ \varphi^T(k) &= [k, 1]. \end{aligned} \tag{13}$$

The least squares fit then is

$$\hat{\theta} = \left[\frac{1}{N}\sum_{k=1}^{N} \varphi(k)\varphi^T(k)\right]^{-1} \frac{1}{N}\sum_{k=1}^{N} y(k)\varphi(k). \tag{14}$$

Dividing the first element in $\hat{\theta}$ with the difference in depths and converting to the proper frequency then yields the attenuation slope.

The standard deviation of the estimate is [28]

$$\begin{aligned} \sigma &= \sqrt{\sigma_e^2 \left(\left[\frac{1}{N}\sum_{k=1}^{N} \varphi(k)\varphi^T(k)\right]^{-1}\right)_{11}} \\ \sigma_e^2 &= \frac{\sum_{k=1}^{N}[y(k) - \hat{\theta}^T\varphi(k)]}{N-2}. \end{aligned} \tag{15}$$

$()_{11}$ denotes the first diagonal element in the matrix.

ACKNOWLEDGMENT

M.Sc. Jan Mathorne built the sampling system for acquiring the images, and M.Sc. Torben Gravesen and Dr. Bjarne Stage wrote the programs for the data acquisition. The scanning was performed at Herlev University Hospital in June 1989 by M.D. Knud-Erik Fredfelt, M.D., Ph.D. Søren Torp-Pedersen, M.D. Christian Noldsø, M. D. Peter Sand Myschetzky, and M.D., Ph.D. Hans-Henrik Holm.

The authors would also like to thank the anonymous reviewers for their numerous, helpful comments.

REFERENCES

[1] J. A. Jensen, "A model for the propagation and scattering of ultrasound in tissue," *J. Acoust. Soc. Am.*, vol. 89, no. 1, pp. 182–191, 1991.
[2] ——, "Medical ultrasound imaging, an estimation based approach," Ph.D. dissertation, Electronic Institute, Technical Univ. Denmark, Sept. 1988.
[3] R. Kuc, "Bounds on estimating the acoustic attenuation of small tissue regions from reflected ultrasound," *Proc. IEEE*, vol. 73, no. 7, pp. 1159–1168, July 1985.
[4] R. B. Kuc, "Application of Kalman filtering techniques to diagnostic ultrasound," *Ultrason. Imag. 1*, pp. 105–120, 1979.
[5] E. E. Hundt and E. A. Trautenberg, "Digital processing of ultrasonic data by deconvolution," *IEEE Trans. Sonics. Ultrason.*, vol. SU-27, no. 5, pp. 249–252, September 1980.
[6] C. Kasai, K. Namekawa, A. Koyano and R. Omoto, "Real-Time Two-Dimensional Blood Flow Imaging using an Autocorrelation Technique," *IEEE Trans. Sonics Ultrason.*, vol. 32, pp. 458–463, 1985.
[7] O. Bonnefous, "Statistical analysis and the time correlation process applied to velocity measurement," in *Proc. IEEE Ultrason. Symp.*, 1989, pp. 887–892.
[8] M. Fatemi and A. C. Kak, "Ultrasonic B-scan imaging: Theory of image formation and a technique for restoration," *Ultrason. Imag. 2*, pp. 1–47, 1980.
[9] G. Demoment, R. Reynaud and A. Herment, "Range resolution improvement by a fast deconvolution method," *Ultrason. Imag. 6*, pp. 435–451, 1984.
[10] J. P. Jones and S. Leeman, "Ultrasonic tissue characterization, a review," *Acta Electronica*, vol. 26, no. 1, pp. 3–31, 1984.
[11] S. Leeman, L. A. Ferrari, J. P. Jones and M. Fink, "Perspectives on attenuation estimation from pulse-echo signals," *IEEE Trans. Sonics Ultrason.*, vol. 31, no. 4, pp. 352–361, 1984.
[12] R. Kuc and H. Li, "Reduced order autoregressive modeling for center-frequency estimation," *Ultrason. Imag. 7*, pp. 244–251, 1985.
[13] L. Y. Shih, C. W. Barnes and L. A. Ferrari, "Estimation of attenuation coefficient for ultrasonic tissue characterization using time-varying state-space model," *Ultrason. Imag. 10*, pp. 90–109, 1988.
[14] F. Towfig, C. W. Barnes and E. J. Pisa, "Tissue classification based on autoregressive models for ultrasound pulse echo data," *Acta Electronica 26*, pp. 95–110, 1984.
[15] L. Hutchins and S. Leeman, "Pulse and impulse response in human tissues," in *Acoustical Imaging 12*, E. A. Ash and C. R. Hill, Eds. NY: Plenum Press, 1983, pp. 459–467.
[16] W. P. Mason, *Electromechanical Transducers and Wave Filters,* Princeton, NJ: Van Nostrand, 1948.
[17] G. S. Kino, *Acoustic Waves. Devices, Imaging, and Analog Signal Processing,* Englewood Cliffs, NJ: Prentice-Hall, 1987.
[18] A. V. Oppenheim and R. W. Schafer, *Digital Signal Processing,* Englewood Cliffs, NJ: Prentice-Hall, 1975.
[19] J. M. Tribolet, *Seismic Applications of Homomorphic Signal processing,* Englewood Cliffs, NJ: Prentice-Hall, 1979.
[20] J. A. Jensen and J. Mathorne, "A sampling system for clinical ultrasound images," in *Proc. Med. Imag. V Sympos., Int. Soc. Optical Eng.*, San Jose, CA, Feb.–Mar. 1991.
[21] J. Mathorne and J. A. Jensen, "A sampling system for clinical ultrasound pictures," Elec. Lab., Tech. Univ. Denmark, Rep. C.1, 1989.
[22] T. Gravesen, J. A. Jensen and B. Stage, "Programs for the acquisition, storage, processing, and display of clinical ultrasound pictures, user's guide," Elec. Lab., Tech. Univ. Denmark, Rep. D.1, 1989.
[23] ——, "Programs for the acquisition, storage, processing and display of clinical ultrasound pictures, Documentation," Elec. Lab., Tech. Univ. Denmark, Rep. D.2A, 1990.
[24] K. J. Parker, M. S. Asztely, R. M. Lerner, E. A. Schenk and R. C. Waag, "*In vivo* measurements of ultrasound attenuation in normal or diseased liver," *Ultrasound in Med. & Biol.*, vol. 14, no. 2, pp. 127–136, 1988.
[25] S. A. Goss, R. L. Johnston and F. Dunn, "Comprehensive compilation of empirical ultrasonic properties of mammalian tissues," *J. Acoust. Soc. Am.*, vol. 64, no. 2, pp. 423–457, 1978.
[26] ——, "Compilation of empirical ultrasonic properties of mammalian tissues. II," *J. Acoust. Soc. Am.*, vol. 68, no. 1, pp. 93–108, 1980.
[27] *Pro-Matlab for Apollo Workstations,* The Math Works, Inc., 1989.
[28] B. Abraham and J. Ledolter, *Statistical Methods of Forecasting,* NY: Wiley, 1983.

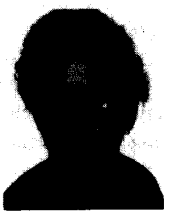

Jørgen Arendt Jensen was born in Roskilde, Denmark, in 1960. He received the M.Sc. degree in electrical engineering in 1985 and the Ph.D. degree in 1989 from the Technical University of Denmark. The subject of his dissertation was digital signal processing in medical ultrasound.

He was a Postdoctoral Fellow at the Electronics Institute at the Technical University of Denmark from 1989 to 1992, and has been a Visiting Scientist at King's College, UK, Duke University, NC, Stanford University, CA, and the Bioacoustics Research Laboratory at the University of Illinois at Urbana-Champaign from 1992 to 1993. He currently holds a three years' Professorship at the Technical University of Denmark. He has published a number of reports and papers on digital signal processing, ultrasound acoustics, and medical ultrasound imaging.

Sidney Leeman, photograph and biography not available at time of publication.